Negative skin friction and the neutral plane

ELMER L. MATYAS AND J. CARLOS SANTAMARINA
Department of Civil Engineering, University of Waterloo, Waterloo, ON N2L 3G1, Canada

Received November 15, 1993
Accepted March 18, 1994

Current views indicate that negative skin friction on piles can be mobilized at small relative deformations and should be considered in all designs, primarily for serviceability conditions. An elastic-plastic closed-form solution is presented that permits an estimate of down-drag forces and the location of the neutral plane. It is shown that the conventional rigid-plastic solution may overestimate down-drag forces by as much as 50% and may also overestimate the depth of the neutral plane.

Key words: piles, negative skin friction, neutral plane, capacity.

L'opinion actuelle est que le frottement latéral négatif sur les pieux peut être mobilisé lors de déformations relatives faibles et devrait être pris en compte dans tous les projets, essentiellement pour les conditions de service. On présente ici une solution élasto-plastique explicite qui permet d'estimer les forces d'adhérence vers le bas et la position du plan neutre. On montre que la solution classique rigide-plastique peut surestimer les forces d'adhérence vers le bas avec un facteur pouvant atteindre 50% et surestimer également la profondeur du plan neutre.

Mots clés : pieux, frottement latéral négatif, plan neutre, capacité portante.

Can. Geotech. J. **31**, 591–597 (1994)

Introduction

Several solutions have been proposed to determine the magnitude and distribution of down-drag forces that may act on a driven pile in soils. For example, the Canadian Geotechnical Society (1985) and Fellenius (1989, 1991) use a relatively simple rigid-plastic model in terms of effective stresses to determine the maximum down-drag force Q_n. The maximum load Q_{NP} that acts on the pile is equal to the applied dead load Q_d plus Q_n and it occurs at the neutral plane, which is defined by depth z_{NP} below the ground surface (Fig. 1). This maximum load must not exceed the allowable structural capacity of the pile.

Poulos and Davis (1975, 1980) provided parametric solutions that considered various factors such as full slip, partially mobilized strength, rigid piles, toe-bearing piles, and shaft-bearing piles. Numerical and closed-form solutions were shown to give reasonable agreement between theory and observations on full-scale piles.

This paper presents a summary of the rigid-plastic model that is frequently used to calculate down drag, the location of the neutral plane, and the axial load in a pile. A solution is then developed in which the soil adjacent to the shaft and below the pile toe is assumed to behave as an elastic-plastic material. Resulting equations are expressed in dimensionless terms to enhance generality and to reduce the number of parameters. The case that is solved is for soil strength increasing linearly with depth. This assumption is compatible with the approximately linear increase of vertical effective stress with depth. The paper includes equations and figures that permit comparisons between the two models.

Induced and applied loads in a pile: Conventional approach

A brief summary of the key components that contribute to the loads acting on a pile is presented below. The summary is based primarily on the Canadian Geotechnical Society (1985) and Fellenius (1989, 1991).

When the soil deposit through which piles have been installed settles, the resulting downward movement of the soil around the piles induces down-drag forces on the piles through negative skin friction. The magnitude of the relative settlement between the soil and the pile needed to cause the negative skin friction is less than a few millimetres. These small relative movements can be induced by reconsolidation of the soil around the pile that is disturbed during installation or by settlement of the soil as a result of the application of a surface fill. The drag load due to negative skin friction at depth z is given by

$$[1a] \quad Q_n = \int_0^z A_s \beta \sigma'_z \, dz$$

and

$$[1b] \quad \beta = MK_s \tan \phi'$$

where A_s is the shaft area per unit length of pile, β is the Bjerrum–Burland coefficient, σ'_z is the vertical effective stress at depth z, M is the quotient of wall friction = $\tan \delta / \tan \phi'$, δ is the soil–pile friction angle, ϕ' is the effective angle of internal friction, and K_s is the lateral earth pressure coefficient. The β coefficient ranges from about 0.25 for clay to about to 0.8 for gravel (Table 1). The ultimate shaft resistance R_{su} is given by

$$[2] \quad R_{su} = \int_0^D A_s \beta \sigma'_z \, dz$$

As with negative skin friction, only small relative movements between the soil and the pile are required to mobilize the full shaft resistance. The ultimate toe resistance R_{tu} is given by

$$[3] \quad R_{tu} = A_t N_t \sigma'_{z=D}$$

where A_t is the cross-sectional area of the pile toe, and N_t is a toe bearing capacity coefficient. N_t ranges from a low value of about 3 for clay to an upper limit of about 300 for gravel (Table 1). The movement of the pile toe that is required to develop the ultimate toe resistance for a driven

Printed in Canada / Imprimé au Canada

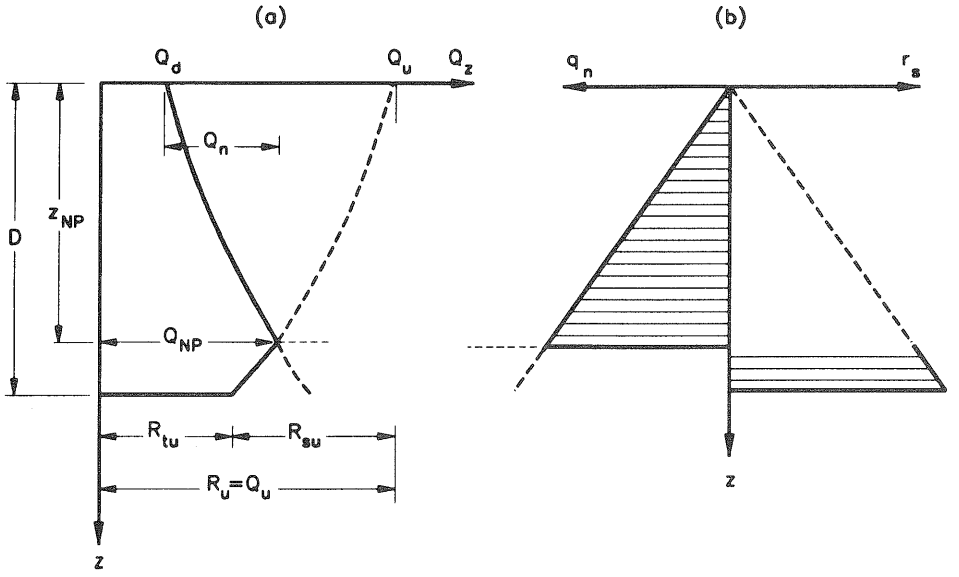

FIG. 1. Rigid-plastic model. (*a*) Axial load distribution, Q_z vs. z. (*b*) Distribution of positive and negative unit shaft resistance, r_s and q_n, respectively.

pile lies in the range of about 3–10% of the pile toe diameter B. The load–movement relationship is not linear.

The neutral plane is located at the depth where the negative skin friction changes over to positive shaft resistance. The location of the neutral plane defines the maximum load in the pile; both the location of the neutral plane and the maximum load are needed to compute the settlement of the pile. For a dominantly shaft-bearing pile (floating pile) in a relatively homogeneous soil, the location of the neutral plane is dependent on the applied load and usually lies at a depth between one-half and two-thirds the embedment depth: the neutral plane moves downward as the toe resistance increases and moves upwards as the dead load increases. In the next section, the location of the neutral plane and the magnitude of the axial load are estimated with a rigid-plastic formulation.

Rigid-plastic model

The rigid-plastic method assumes a rigid-plastic stress–strain response for the soil resistance along the shaft and below the pile toe. Accordingly, it follows that the negative skin friction, positive shaft resistance, and toe resistance, are fully mobilized. An additional consequence is that there is a discontinuity at the neutral plane (Fig. 1). For a given depth, it is usually assumed that the unit negative skin friction q_n is equal to the positive shaft resistance r_s. While this assumption is debatable, it results in an overestimation of the down-drag load (Fellenius 1989).

Two dimensionless ratios α and F_s are introduced:

$$[4a] \quad \alpha = \frac{R_u}{R_{su}}$$

$$[4b] \quad F_s = \frac{R_u}{Q_d}$$

where α is the ratio of ultimate load R_u to ultimate shaft resistance R_{su}, and F_s is the conventional factor of safety in working stress design (WSD) defined as the ratio of ultimate resistance load R_u to applied load Q_d. If q_n and r_s are approximated by a linear function q_n or $r_s = a\,z$, where a is a constant, and z is the depth below the surface, the rigid plastic model predicts

$$[5a] \quad \frac{z_{NP}}{D} = \sqrt{\frac{\alpha}{2}\left(1-\frac{1}{F_s}\right)}$$

$$[5b] \quad \frac{Q_{NP}}{R_u} = \frac{1}{2}\frac{(1+F_s)}{F_s}$$

where D is the depth of pile embedment.

Elastic-plastic model

For the elastic-plastic method, a simple closed-form solution is developed that permits an estimate of the negative skin friction in terms of the most relevant parameters. Shaft and toe resistances are characterized by means of elastic-plastic soil models, where δ_{sy} is the displacement of the soil relative to the pile that is required to yield the shaft resistance (Fig. 2*d*), and δ_{ty} is the displacement that yields the toe resistance (Fig. 2*e*). Subscripts s, t, y, and m are used to indicate shaft, toe, yield, and mobilized, respectively. The relative displacement profile (Fig. 2*a*) is assumed linear, with maximum value at the ground surface and decreasing with depth. The pile is assumed to be rigid.

Three additional dimensionless ratios ψ, ω, and λ are introduced:

$$[6a] \quad \psi = \frac{\delta_{ty}}{S}$$

$$[6b] \quad \omega = \frac{\delta_{sy}}{S}$$

$$[6c] \quad \lambda = \frac{\delta_h}{S}$$

These dimensionless parameters are relative displacements normalized with respect to the total relative settlement $S = \delta_h + \delta_t$, where δ_h is the settlement of the pile head relative to the ground surface, and δ_t is the relative settlement of the pile toe. The settlement S is given by the integral

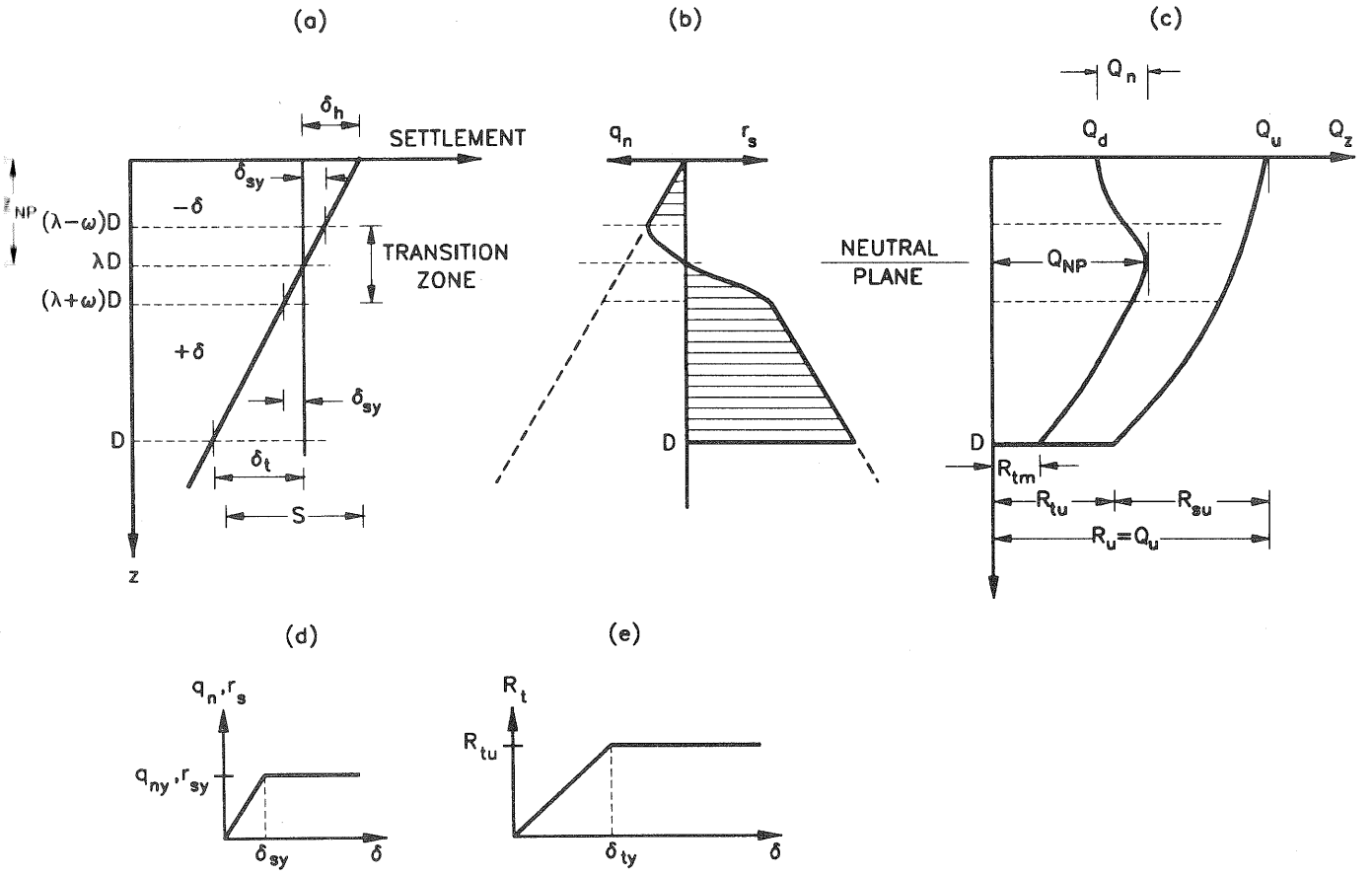

FIG. 2. Elastic-plastic model. (*a*) Relative displacements. (*b*) Distribution of unit shaft resistance. (*c*) Load distribution. (*d*) Mobilization of shaft resistance. (*e*) Mobilization of toe resistance. δ, relative displacement; $S = \delta_h + \delta_t$; q_{ny} and r_{sy} are the negative and positive unit shaft resistance at yield; R_t, toe resistance.

of the vertical strain in the soil mass within the depth of embedment D.

Compatibility of relative deformations along the pile results in three zones (Fig. 2): fully mobilized negative skin friction in the upper zone, where $|\delta_z| < \delta_{sy}$; a transition zone where $|\delta_z| > \delta_{sy}$; and a lower zone where $\delta_z > \delta_{sy}$. The purpose of the calculation is to evaluate the settlement of the pile relative to the soil that verifies equilibrium, therefore

$$[7] \quad Q_d + \int_0^{(\lambda-\omega)D} A_s q_{ny}\, dz + \int_{(\lambda-\omega)D}^{\lambda D} A_s q_{nzm}\, dz = \int_{\lambda D}^{(\lambda+\omega)D} A_s r_{szm}\, dz + \int_{(\lambda+\omega)D}^{D} A_s r_{sy}\, dz + R_{tm}$$

After integration, all terms were normalized with respect to the ultimate shaft resistance R_{su}, and the resulting equation was solved for λ:

$$[8] \quad \lambda = \frac{\sqrt{(\alpha-1)^2 + 8\psi(\alpha-1) + 8\psi^2\left(1 - \frac{\alpha}{F_s} - \frac{2\omega^2}{3}\right)} - (\alpha-1)}{4\psi}$$

From the geometry of displacements in Fig. 2, it may be noted that λ is also the normalized location of the neutral plane, that is,

$$[9] \quad \lambda = \frac{\delta_h}{S} = \frac{z_{NP}}{D}$$

The integral of forces above the neutral plane results in

$$[10] \quad \frac{Q_{NP}}{R_u} = \frac{1}{\alpha}\left(\lambda^2 - \lambda\omega + \frac{1}{3}\omega^2\right) + \frac{1}{F_s}$$

The length of the pile between $(\lambda - \omega)D$ and $(\lambda + \omega)D$ is the extent of the transition zone t_{trans} between fully mobilized negative skin friction and fully mobilized positive shaft resistance (3rd and 4th terms in [7]), that is,

$$[11] \quad t_{trans} = 2\omega D = 2\frac{\delta_{sy}}{S} D$$

The elastic-plastic analysis, therefore, predicts that the thickness of the transition zone decreases as the stiffness of the shaft resistance and (or) the compressibility of the soil increases.

The validity of these equations is limited to the case where the transition zone is fully contained within the length D of the pile, and for $\delta_t < \delta_{ty}$, that is,

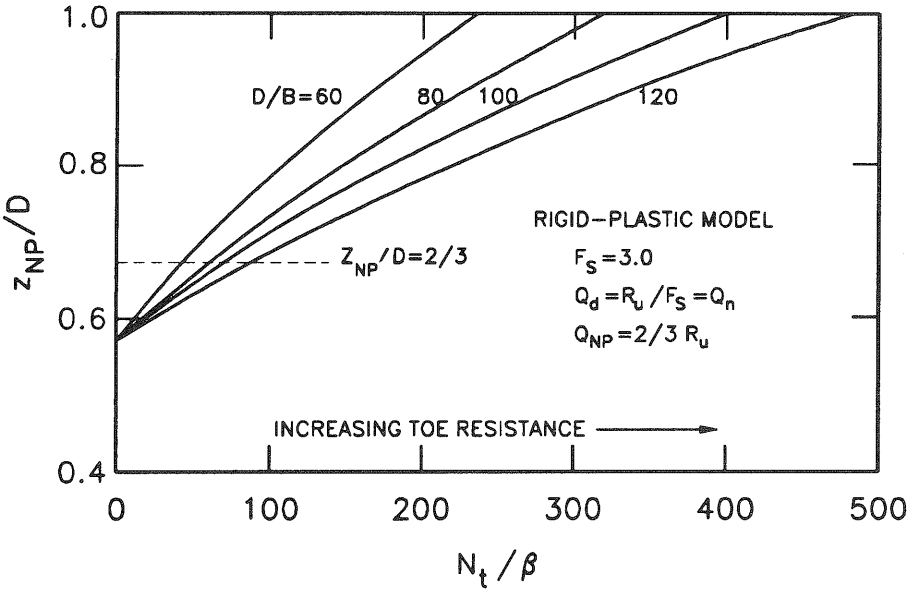

FIG. 3. Rigid–plastic model. Normalized depth to neutral plane vs. resistance ratio (N_t/β) for different D/B ratios.

TABLE 1. Ranges of ϕ, β, and N_t values

Soil type	ϕ (°)	β	N_t
Clay	25–30	0.25–0.35	3–30
Silt	28–34	0.27–0.50	20–40
Sand	32–40	0.30–0.60	30–150
Gravel	35–45	0.35–0.80	60–300

NOTE: From Ontario Highway Bridge Design Code (1992).

[12*a*] $0 < \lambda - \omega$

[12*b*] $\lambda + \omega < 1$

[12*c*] $\lambda + \psi > 1$

When the full toe resistance is mobilized ($\lambda + \psi = 1$) and the deformation to yield the shaft is nil ($\omega = 0$), then [8] and [10] become [5*a*] and [5*b*], respectively, and show that the rigid-plastic solution is a special case of the elastic-plastic solution.

Comparison of rigid-plastic and elastic-plastic models

To facilitate comparisons between the two models, criteria common to geotechnical practice were included. Combining [2] and [3] with [4*b*] gives

$$[13] \quad \alpha = \frac{N_t/2\beta}{D/B} + 1$$

where B is the diameter of the pile. The ratio D/B is likely to range from about 10 for short piles to about 100 or more for long piles. From Table 1, the ratio N_t/β ranges from about 10 to 1000. In conventional working stress design, a factor of safety of 3.0 is usually applied to calculated pile capacities whereas a lower value of 2.0 may be adopted if reliable pile loading test data are available. For the determination of the depth to the neutral plane, the live load $Q_l = 0$. The dead load Q_d must be unfactored in both WSD and limit states design (LSD). For the stated assumptions, [5*b*] gives a unique value of $Q_{NP} = 2R_u/3$ for $F_s = 3.0$.

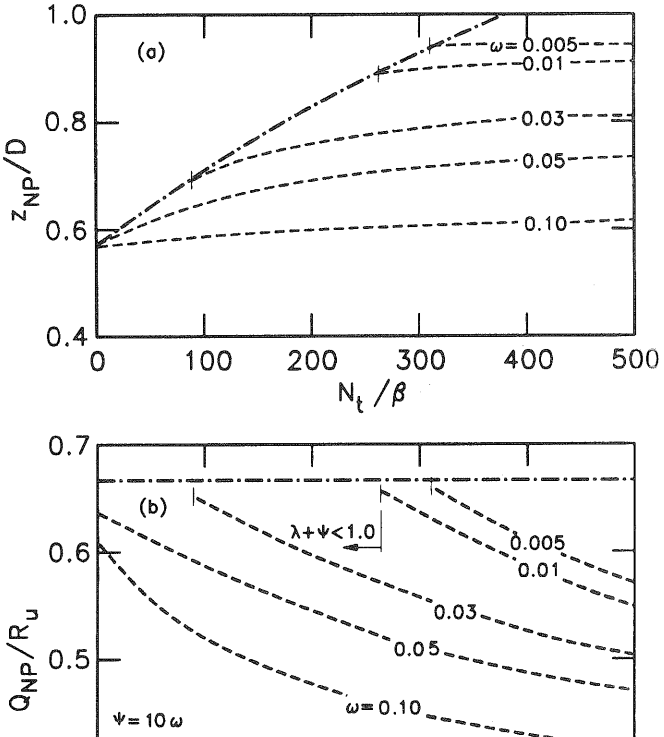

FIG. 4. Model comparison. (*a*) Normalized depth ratio vs. resistance ratio (N_t/β). (*b*) Normalized load vs. resistance ratio (N_t/β).

Rigid-plastic model

Equations [5*a*], [5*b*], and [13] were combined and used to prepare Fig. 3. The ratio D/B was limited to a range of 60–120, since down-drag forces are likely to be of concern

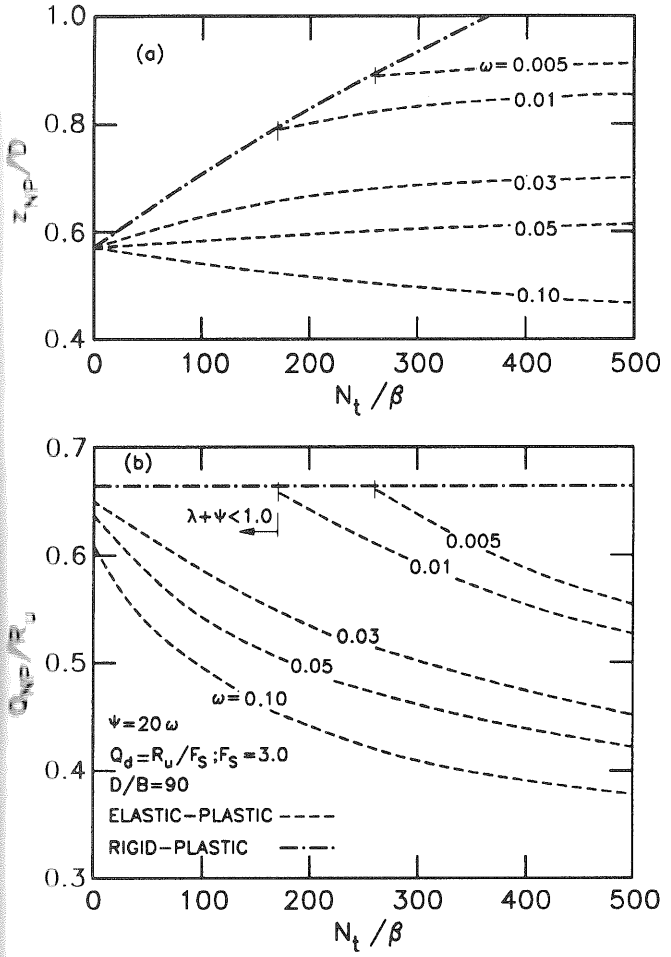

FIG. 5. Model comparison. (*a*) Normalized depth ratio vs. resistance ratio (N_t/β). (*b*) Normalized load vs. resistance ratio (N_t/β).

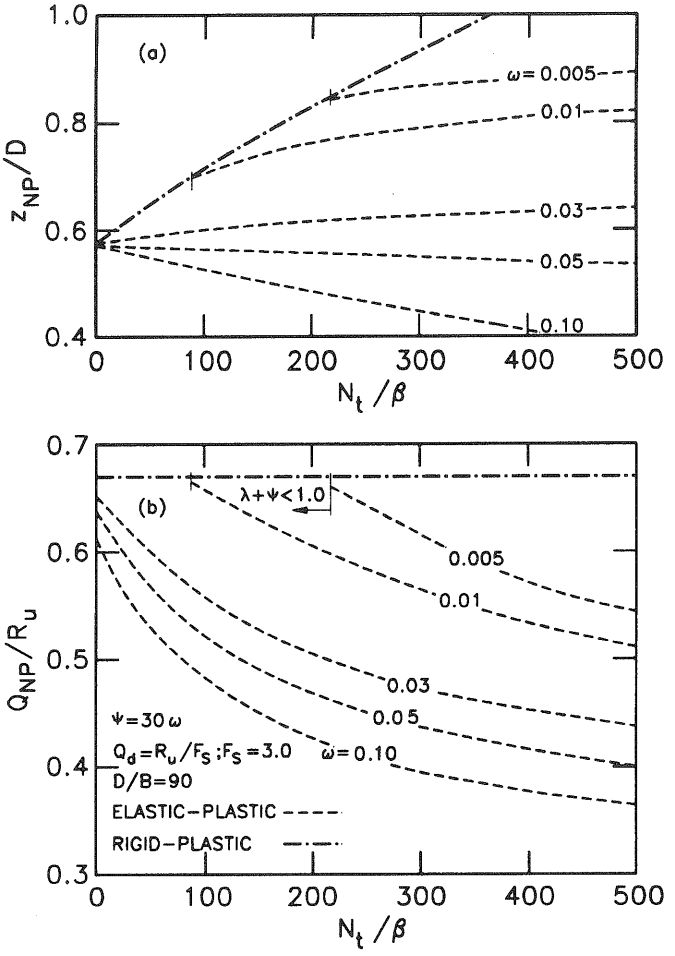

FIG. 6. Model comparison. (*a*) Normalized depth ratio vs. resistance ratio (N_t/β). (*b*) Normalized load vs. resistance ratio (N_t/β).

TABLE 2. Results for numerical examples

					Rigid-plastic model			Elastic-plastic model		
	F_s	N_t/β	R_u (kN)	Q_d (kN)	z_{NP} (m)	Q_{NP} (kN)	Q_n (kN)	z_{NP} (m)	Q_{NP} (kN)	Q_n (kN)
Equation			[2] + [3]	[4*b*]	[5*a*]	[5*b*]	[5*b*] − [4*b*]	[8]	[10]	[10] − [4*b*]
Pile 1	3.0	12	915	305	16.1	610	305	15.6	570	265
Pile 2	3.0	400	2770	925	27.0	1845	920	16.7	1225	300
Pile 1	2.0	12	915	460	13.9	690	230	13.5	650	190
Pile 2	2.0	400	2770	1385	24.2	2080	695	13.5	1580	195

NOTE: In each example the elastic-plastic model (eq. [11]) gives a thickness of 2.7 m for the transition zone.

only for relatively long piles. As shown, the depth to the neutral plane increases as the toe resistance increases and, depending on the *D*/*B* ratio, reaches a normalized value of 1.0 at an N_t/β ratio between approximately 250 and 500. It is often suggested that for dominantly shaft-bearing piles (low N_t/β ratio), the neutral plane lies at a depth that is about equal to the lower third point of the pile embedment depth. As indicated in Fig. 3, this criterion is met at specific combinations of N_t/β and *D*/*B*.

Elastic-plastic model

For a common pile diameter of 300 mm, movements of about 10–30 mm are required to mobilize toe resistance whereas only a few millimetres are sufficient to yield the shaft resistance. Thus, from [6*a* and 6*b*], the ratio ψ/ω is about 10–30. In general, the magnitude of ω will be small because $\delta_{sy} \ll S$. Equations [8] and [10] can be readily evaluated for various combinations of ψ/ω, ω, and *D*/*B* and plotted as shown in Figs. 4–6. These figures are based on *D*/*B* = 90 and are used to illustrate the rigid–plastic and elastic-plastic models with numerical examples which follow. As shown, some curves terminate as a consequence of the limits of the solution given by [12].

Numerical examples

Consider a clay deposit with the water table at the ground surface. Let buoyant unit weight $\gamma' = 10$ kN/m^3 and $\beta = 0.25$. The toe of pile 1 is installed in clay with $N_t = 3$, and

the toe of pile 2 is installed in a dense soil with $N_t = 100$. Each cylindrical pile has an embedded length $D = 27$ m and a diameter $B = 0.3$ m. From [2], $R_{su} = 860$ kN, and from [3] $R_{tu} = 60$ and 1910 kN for piles 1 and 2, respectively. For the elastic–plastic solution, it is assumed that (*i*) the settlement of the clay deposit within the length of the pile is 20 mm, (*ii*) a relative settlement of about 1.0 mm is needed to mobilize the shaft resistance and (*iii*) a movement of 20 mm is needed to mobilize the toe resistance. From [6*b*], $\omega = 0.05$; [6*a* and 6*b*] give $\psi/\omega = 20$. The loads in each pile and the depth to the neutral plane can be obtained through Fig. 5 for $F_s = 3.0$; results are summarized in Table 2. For comparison, results are also given for $F_s = 2.0$. In each example, the elastic-plastic solution (Eq. [11]) gives a thickness of 2.7 m for the transition zone.

For the stated assumptions, these examples illustrate that the rigid-plastic and elastic-plastic models give similar results for pile 1 because the pile toe is in relatively low strength soil. However, for pile 2, which has a high toe coefficient N_t, the calculated load at the neutral plane is about 50% higher than the calculated load based on the elastic-plastic model. This difference reduces to about 30% when the factor of safety is 2.0. For pile 2, the down-drag force $Q_n = Q_{NP} - Q_d$ is significantly greater for the rigid-plastic model.

Limitations and consequences of the model's assumptions

Pile stiffness

In the transition zone, the relative stiffness between the soil and the pile would be expected to alter the results. Parametric studies conducted by other authors, however, show that the effect of relative stiffness is minor, e.g., Poulos and Davis (1980). As indicated in Figs. 4–6, the results are more likely to be influenced by uncertainties in the magnitudes of ψ and ω. This is more evident at increasing values of ψ and decreasing values of toe resistance.

Nonlinear soil settlement

Consolidating soil adjacent to the pile is likely to produce strains that are nonlinear and decrease with depth approximately given by $\epsilon_z = f(z^{-0.5})$. However, within the transition zone, a linear relationship can be assumed in most cases.

Negative and positive yield shaft resistance

The magnitude of the negative unit yield shaft resistance is likely to be lower than the positive unit shaft resistance as a consequence of a number of factors that includes changes in effective stress as a result of installation and (or) consolidation. This effect could be modelled approximately by assuming a reduction factor in the integrals on the left-hand side of [7] and would result in a reduction of calculated load at the neutral plane. Following Fellenius (1989), the assumption of equal negative and positive unit yield shaft resistance is conservative because it results in an overestimate of the drag load and places the neutral plane at a higher elevation.

Variations of δ_{sy}

The behaviour of the soil, e.g., contractive vs. dilative, will be influenced by the current magnitude of the effective stresses at a given depth and will lead to changes in δ_{sy}. Compounding factors such as pile installation and uncertainty in S dissuade further refinement.

Variation of r_s

In many practical situations, the soil profile is layered, the upper portion of the soil deposit is overconsolidated due to desiccation, etc., and therefore the variation of r_s is nonuniform. General closed-form solutions to include these factors are not warranted.

Construction history

The load-transfer mechanism in a pile is affected by pile driving and loading history. In these analyses, it was assumed that the pile had no residual stresses due to installation; therefore, if residual loads were present, they would be added to the calculated loads to obtain the actual loads. Also, the sequence of loading, e.g., the addition of a dead load before, or after, the mobilization of the drag load would alter the distribution of load in the pile. This, and other limitations discussed above, can be readily modelled in numerical solutions for specific cases. Still, closed-form solutions presented in this note highlight trends and the significance of the most relevant parameters.

Conclusions

Simple expressions were derived to determine the location of the neutral plane (eq. 8), the load at the neutral plane resulting from down drag plus applied loads (eq. 10), and the thickness of the transition zone (eq. 11). The pile was assumed to be rigid and embedded within a medium with linearly increasing shaft resistance. These expressions show that conventional rigid-plastic models can overestimate the value of the maximum axial load by 50% or more and overpredict the depth of the neutral plane.

Canadian Geotechnical Society. 1985. Canadian foundation engineering manual. 2nd ed. BiTech Publishers, Vancouver.

Fellenius, B.H. 1989. Unified design of piles and pile groups. Transportation Research Record, No. 1169, pp. 75–82.

Fellenius, B.H. 1991. Pile foundations. Chap. 13. *In* Foundation engineering handbook. 2nd ed. *Edited by* H.Y. Fang. pp. 511–536.

Ontario Highway Bridge Design Code. 1992.

Poulos, H.G., and Davis, E.H. 1975. Prediction of downdrag forces in endbearing piles. ASCE Journal of the Geotechnical Engineering Division, **101**(GT2): 189–204.

Poulos, H.G., and Davis, E.H. 1980. Pile foundation analysis and design. John Wiley & Sons, Inc., Toronto.

List of symbols

A_s	shaft area per unit length of pile
A_t	cross-sectional area of pile toe
B	pile diameter
D	depth of pile embedment
F_s	factor of safety
K_s	lateral earth pressure coefficient
M	quotient of wall friction
N_t	toe bearing capacity coefficient (Table 1)
Q_d	applied dead load
Q_n	drag load
Q_{NP}	load at neutral plane
Q_u	ultimate applied load
q_n	unit negative skin friction
R_u	ultimate resistance
R_t	toe resistance
R_{sm}	mobilized shaft resistance
R_{su}	ultimate shaft resistance
R_{tm}	mobilized toe resistance

R_{tu}	ultimate toe resistance	σ'_z	vertical effective stress at depth z
f_s	unit positive shaft resistance	ϕ'	effective angle of internal friction
S	total relative settlement	δ_{sy}	relative displacement that yields the shaft resistance
l_{trans}	extent of the transition zone	δ_{ty}	relative displacement that yields the toe resistance
z	depth below ground surface	δ_h	relative settlement of the pile head
z_{NP}	depth to neutral plane	δ_t	relative settlement of the pile toe
α	dimensionless load ratio	δ_z	relative displacement at depth z
β	shaft resistance coefficient	γ	unit weight of soil
λ, ψ, ω	dimensionless relative settlement ratios	γ'	buoyant unit weight of soil

Tension tests on bored piles in cemented desert sands

NABIL F. ISMAEL, HASAN A. AL-SANAD, AND FAHAD AL-OTAIBI

Civil Engineering Department, Kuwait University, P.O. Box 5969, 13060 Safat, Kuwait

Received August 12, 1993

Accepted March 29, 1994

The load transfer of bored piles in medium dense cemented sands was examined by field tests at two sites. At the first site, two bored piles were tested in axial tension to failure. One pile was instrumented with strain guages to measure the axial load distribution at all load increments. The results indicate significant load transfer along the pile length. The average shaft resistance measured was 80 and 100 kN/m^2 in medium-dense and very dense, weakly cemented calcareous sand, respectively. At the second site, a tension test was carried out on a bored pile in uncemented cohesionless sand. By comparing the results at the two sites the influence of cementation on the uplift capacity was assessed. The shaft resistance depends on many factors including the relative density, degree of cementation, soil fabric, and method of construction. It increases with the standard penetration test (SPT) N values; however, the SPT is not considered a reliable test for strength characterization of cemented sands. Analysis of the pile capacity can be made considering both components of soil strength, namely, cohesion intercept c and angle of shearing resistance ϕ.

Key words: bored piles, cemented sands, uplift capacity, friction, shaft resistance.

Le transfert de charge le long de pieux forés dans des sables cimentés moyennement denses a été examiné sur deux sites avec des essais en place. Sur le premier site, deux pieux forés ont été amenés à la rupture par tension axiale. L'un des pieux était instrumenté avec des capteurs de contrainte pour mesurer la répartition de la charge axiale pour chaque incrément de chargement. Les résultats indiquent un transfert de charge significatif sur la longueur du pieu. La résistance moyenne mesurée le long du fût a été de 80 et 100 kN/m^2 dans des sables calcaires cimentés de densité moyenne et forte, respectivement. Sur le deuxième site, on a fait un essai de tension sur un pieu foré dans un sable sans cohésion non cimenté. En comparant les résultats des deux sites on a pu évaluer l'influence de la cimentation sur la résistance à l'arrachement. La résistance le long du fût dépend de nombreux facteurs dont la densité relative, le degré de cimentation, la texture du sol et la méthode de construction. Elle augmente avec l'indice N de l'essai de pénétration standard SPT qui n'est pourtant pas considéré comme fiable pour la caractérisation des sables cimentés. L'analyse de la capacité d'un pieu peut être faite en partant des deux composantes de la résistance du sol, soit l'intercept de cohésion, c, et l'angle de résistance au visaillement, ϕ.

Mots clés : pieux forés, sables cimentés, capacité à l'arrachement, frottement, résistance de fût.

[Traduit par la rédaction]

Can. Geotech. J. **31**, 597–603 (1994)

Introduction

Cemented sands exist in many places of the world where arid or semiarid conditions prevail. These include the Arabian Peninsula (Oweis and Bowman 1981), the south-western United States and Mexico (Beckwith and Hansen 1982), the Indian continental shelf (Datta et al. 1982), South Africa and South West Africa (Netterberg 1982), and Western Australia (Beringen et al. 1982). The excess of evaporation over rainfall leads to the precipitation of cementing agents, mainly carbonates and sulphates, and the formation of crusts of cemented sands.

With development of these areas in connection with oil and mineral exploration, many projects were constructed on land with bored-pile foundations. In Kuwait, these projects include transmission tower lines, heavy multistory buildings, and reinforced concrete slabs of depressed highway sections located below the groundwater level. As a result, interest in the geotechnical properties and the load-transfer mechanism of bored and driven piles in these soil deposits has increased. It has been established that bored piles offer substantial load transfer in cemented calcareous sands in comparison with driven piles (McClelland 1974; Ismael and Al-Sanad 1986; Murff 1987; Ismael 1989, 1990). Moreover, few problems occur during their construction, since no caving occurs and the required depth can be easily reached by augering.

Printed in Canada / Imprimé au Canada